Electronic Supplementary Material (ESI) for Physical Chemistry Chemical Physics.
This journal is © the Owner Societies 2020

Supporting Information

When is Bell-Evans-Polanyi principle fulfilled in Diels-alder reactions on fullerenes?

Paula Pla[1], Yang Wang[2], and Manuel Alcamí[1,3,4]

[1] *Departamento de Química, Universidad Autónoma de Madrid, Módulo 13, 28049 Madrid, Spain.*
[2] *School of Chemistry and Chemical Engineering, Yangzhou University, Yangzhou, Jiangsu 225002, China*
[3] *Instituto Madrileño de Estudios Avanzados en Nanociencia (IMDEA-Nanociencia), 28049 Madrid, Spain*
[4] *Institute for Advanced Research in Chemical Sciences (IAdChem), Universidad Autónoma de Madrid, 28049 Madrid, Spain*

Contents

1 Computational details and functional benchmarking

DFT calculations of reactants, products and transition states (TSs) were optimized using M06-2X/6-31G(d,p)[1] level of theory with the Gaussian 09 program package.[2] The QST2 algorithm, in which the geometry of the products and reactants is given, was used to search and optimize TSs. Frequency and IRC calculations have been done to ensure that the TSs found were first order saddle points (one imaginary frequency) and that the located TSs were connected to the corresponding products. Also they were used to obtain energies for the reactant complexes on selected adducts. NICS and TDDFT calculations have been performed at the same M06-2X/6-31G(d,p) level of theory with Gaussian 09 program package. Maximum bonding fragment orbital (MBFO) analysis[3] was conducted to reveal the frontier orbital interactions between the diene and the fullerene fragments in the whole system at the geometry of the TS. Nomenclature of fullerene isomers follows the Fowler-Manolopoulos ring spiral algorithm.[4]

Fullerenes C_{70} (1) and C_{80} (6) were chosen as a test case to ensure that the trends obtained in this study do not vary with the functional chosen. Figure S1 shows the correlation between reaction energy and energy barriers of C_{70} (1) and C_{80} (6) using functionals M06-2X, B3LYP and BP86 with 6-31G(d,p) basis set. The same trends are observed independently of the functional, but the M06-2X was chosen due to the incorporation of at least, some dispersion. This functional has been used in previous studies of the DA reaction in fullerenes.[5] TS of adduct **4** of C_{80} (6) using BP86 was not possible to optimize due to the tiny HOMO-LUMO gap.[6]

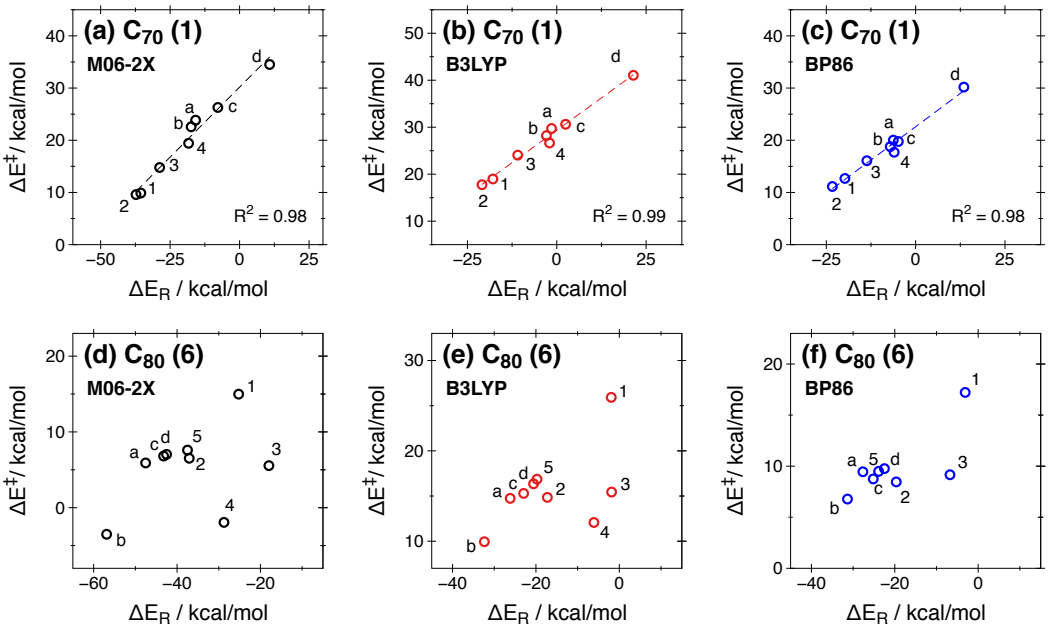

Figure S1: Benchmark of functionals M06-2X, B3LYP and BP86 for fullerenes C_{70} (1) and C_{80} (6).

2 Geometrical parameters of transition states of C_{68} (6290) and C_{76} (1)

Table S1 and S2 show the distances of the C–C bonds that are being formed during the DA reaction in the optimized geometry of the TS for C_{76} (1) and C_{68} (6290), respectively. The mean of the two distances is also presented in the last column.

Table S1: C–C distances of the two bonds that are formed during the DA reaction for adducts of C_{76} (1) in the optimized geometry of the TS.

Isomer	**Distance 1 (Å)**	**Distance 2 (Å)**	**Mean distance (Å)**
1	2.2707	2.2629	2.2668
2	2.2620	2.2131	2.2376
3	2.2597	2.2565	2.2581
4	2.2556	2.2767	2.2662
5	2.0793	2.3140	2.1967
6	2.1720	2.2205	2.1963
7	2.2581	2.1792	2.2187
8	2.3155	2.0909	2.2032
9	2.2576	2.1679	2.2128
10	2.0608	2.2775	2.1692
11	1.9444	2.4251	2.1848
12	1.9495	2.3805	2.1650
13	2.0830	2.2605	2.1718
14	2.3650	1.9777	2.1714
15	2.1070	2.2133	2.1602
16	2.2551	2.0156	2.1354
17	1.9238	2.3721	2.1480
18	2.3684	1.7369	2.0527
19	2.4492	1.7966	2.1229
20	2.2165	2.0592	2.1379
21	1.8296	2.4211	2.1254
22	2.0740	2.1697	2.1219
23	1.9675	2.2301	2.0988
24	1.9670	2.2819	2.1245
25	2.1427	2.1241	2.1334
26	2.0098	2.1710	2.0904
27	2.4255	1.7922	2.1089
28	2.2097	1.8167	2.0132
29	1.8455	2.2367	2.0411
30	1.9854	2.1048	2.0451

Table S2: C–C distances of the two bonds that are formed during the DA reaction for adducts of C_{68} (6290) in the optimized geometry of the TS.

Isomer	Distance 1 (Å)	Distance 2 (Å)	Mean distance (Å)
1	2.1794	2.4852	2.3323
2	2.4761	2.1778	2.3270
3	1.6916	2.6193	2.1555
4	2.3007	2.2226	2.2617
5	2.9634	1.8828	2.4231
6	2.2554	2.2549	2.2552
7	2.2923	2.2370	2.2647
8	2.8769	1.8585	2.3677
9	2.2311	2.3024	2.2668
10	2.2360	2.2368	2.2364
11	2.2332	2.2321	2.2327
12	2.1288	2.3073	2.2181
13	2.0625	2.4062	2.2344
14	2.2213	2.2213	2.2213
15	2.1831	2.2519	2.2175
16	2.6305	1.9361	2.2833
17	2.1888	2.1750	2.1819
18	2.1446	2.2571	2.2009
19	2.7026	1.8815	2.2921
20	2.4014	1.9694	2.1854
21	2.0119	2.3156	2.1638
22	1.8182	2.9114	2.3648
23	2.2969	2.0080	2.1525
24	1.8546	2.7441	2.2994
25	2.2940	2.0223	2.1582
26	1.9896	2.3571	2.1734
27	1.9833	2.3377	2.1605
28	2.1996	2.0873	2.1435
29	2.3093	1.9750	2.1422
30	2.3950	1.8905	2.1428
31	2.6174	1.7475	2.1825
32	2.5584	1.7692	2.1638
33	2.4263	1.8633	2.1448
34	2.0641	2.1710	2.1176
35	2.3857	1.8074	2.0966
36	1.7336	2.4100	2.0718
37	2.0738	2.2015	2.1377
38	2.1428	2.1423	2.1426
39	1.7478	2.5667	2.1573
40	2.1260	2.0791	2.1026
41	2.3937	1.8373	2.1155
42	2.3831	1.9063	2.1447
43	1.8757	2.4317	2.1537
44	2.0033	2.2541	2.1287
45	2.1413	2.0911	2.1162
46	1.9819	2.1724	2.0772
47	1.8564	2.3392	2.0978
48	1.7784	2.4333	2.1059
49	1.9420	2.2015	2.0718
50	2.2106	1.7576	1.9841
51	2.2532	1.8790	2.0661
52	2.0284	2.0222	2.0253

3 Correlation between reaction energies and reaction enthalpies and reaction Gibbs free energies

Figure S2 shows that the trends in the results obtained for reaction energies are also maintained when studying reaction enthalpies and reaction Gibbs free energies.

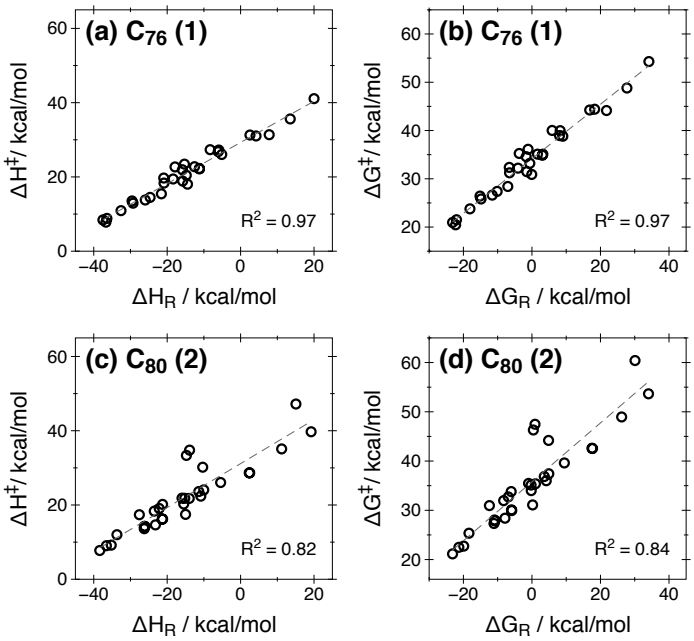

Figure S2: Correlation between reaction energy and reaction enthalpy of a) C_{76} (1) and c) C_{80} (2) and between reaction energy and reaction Gibbs free energy of b) C_{76} (1) and d) C_{80} (2).

4 Correlation between HOMO–LUMO gap and R^2

Figure S3 shows the correlation between HOMO–LUMO gap and R^2 for all fullerenes considered in this article (data of Table 1).

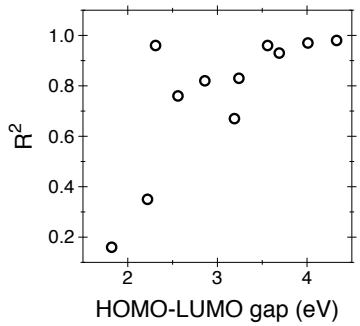

Figure S3: Correlation between HOMO–LUMO gap and correlation coefficient R^2 of all fullerenes considered.

5 Correlations for other fullerenes

Figure S4 shows the correlation between the reaction energy and energy barrier for the other fullerenes discussed in the main article.

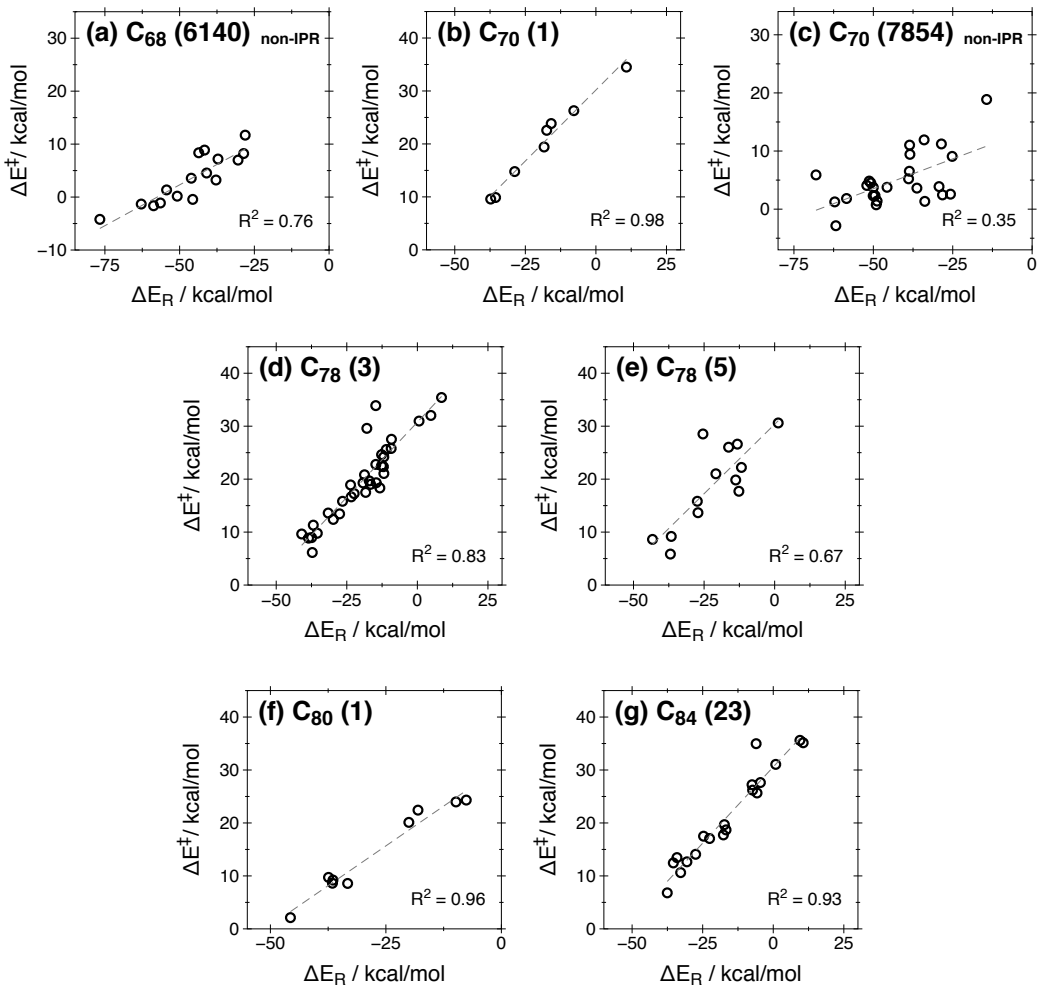

Figure S4: Correlations between reaction energies and energy barriers for all possible regioisomers of fullerenes a) C_{68} (6140), b) C_{70} (1), c) C_{70} (7854), d) C_{78} (3), e) C_{78} (5), f) C_{80} (1) and g) C_{84} (23).

6 Correlation of C_{70} (7854)

Figure S5 shows correlation of C_{70} (7854) including all possible adducts found (left) and only showing the [4+2] adducts confirmed by the IRC (Intrinsic Reaction Coordinate) calculation (right).

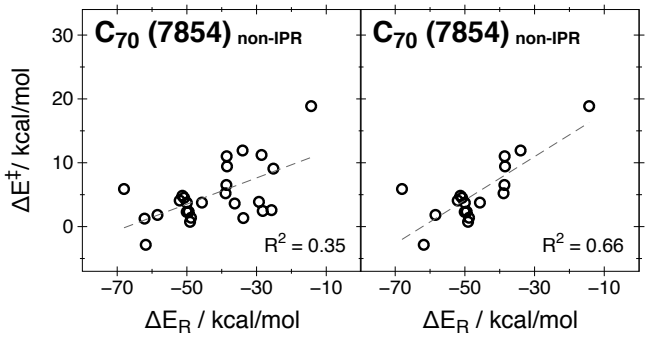

Figure S5: Correlation between reaction energies and energy barriers for C_{70} (7854) including all possible adducts found (left) and only showing [4+2] adducts (right).

7 Schlegel diagrams

Figure S6 shows Schlegel diagrams of selected fullerenes. Regioisomers that have been mentioned are highlighted in each case.

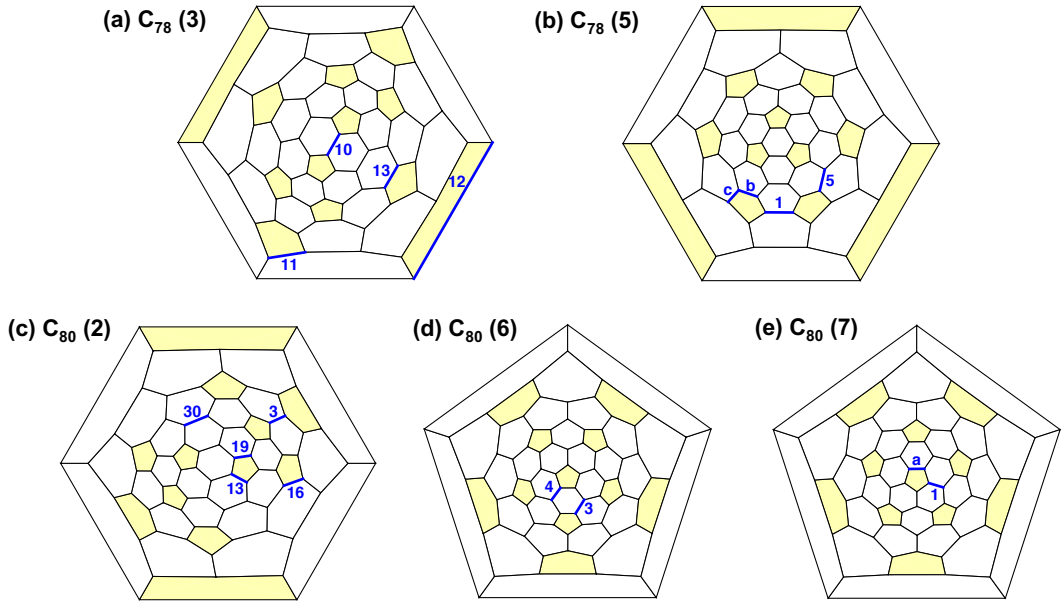

Figure S6: Schlegel diagrams of fullerenes a) C_{78} (3), b) C_{78} (5), c) C_{80} (2), d) C_{80} (6) and e) C_{80} (7).

8 Difference of NICS between adduct and empty cage at 1 Å above the center of each ring for C_{80} (2)

Figure S7 shows the difference of NICS at 1 Å above the center of each ring for selected adducts of C_{80} (2). Note that the difference of NICS for adducts **3**, **10** and **22** is smaller than for adducts **16**, **19** and **30** that are the ones that deviate from the correlation.

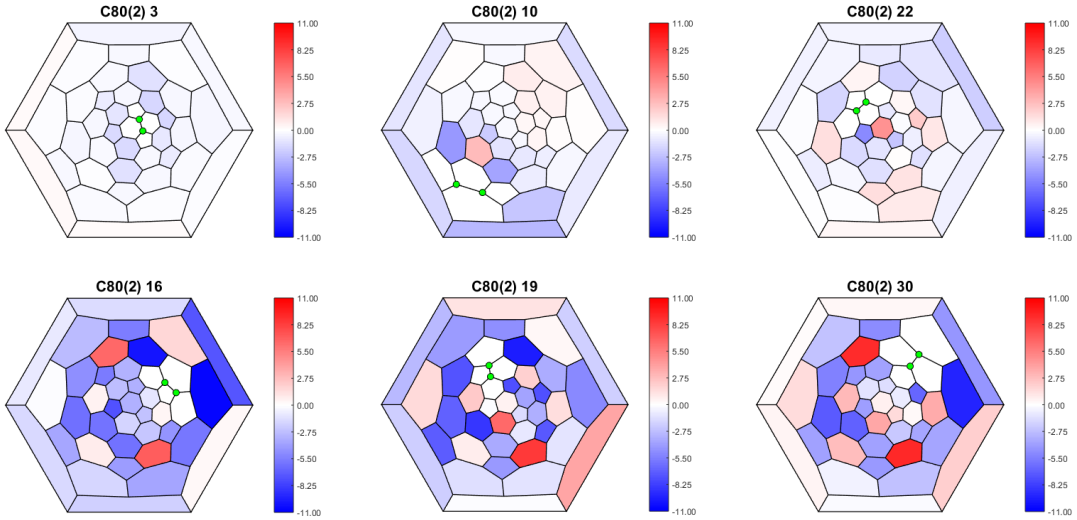

Figure S7: Difference of NICS at 1 Å above the center of each ring for selected adducts of C_{80} (2). The two carbon atoms where the addition is taking place are marked with green circles. The four rings that surround the bond where the addition is taking place are set to zero.

9 Correlation, NICS and molecular orbitals of C_{78} (3)

Figure S8 shows correlation, NICS and molecular orbitals of C_{78} (3). The same conclusions of Figure 4 of the main article can be drawn.

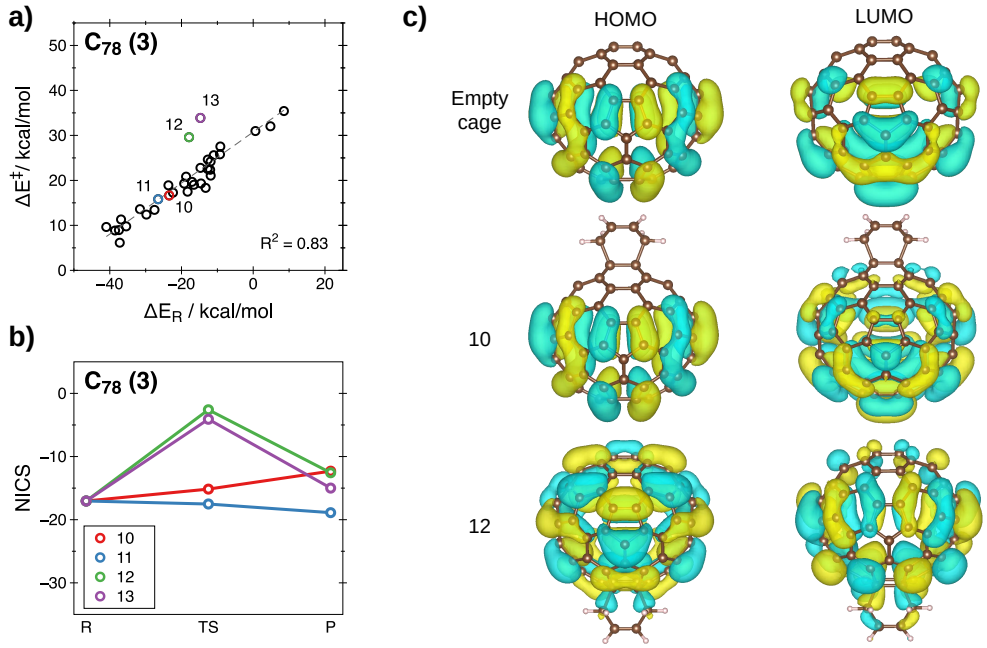

Figure S8: a) Correlation between reaction energies and energy barriers for all possible regioadducts formed by DA addition of 1,3-butadiene with fullerene C_{78} (3). b) Evolution of the NICS value in the center of the cage during DA reaction of 1,3-butadiene with fullerene C_{78} (3) for some adducts. c) HOMO and LUMO orbitals for selected adducts (**10** and **12**) and for the empty cage.

10 Correlation, NICS and molecular orbitals of C_{78} (5)

Figure S9 shows correlation, NICS and molecular orbitals of C_{78} (5). In this case, molecular orbitals are more mixed than in other cases and the correlation coefficient between reaction energies and energy barriers is not that good. For instance, HOMO of adduct **b** is HOMO-1 of the empty cage. Note that adduct **c** which has the HOMO and the LUMO orbitals exchanged, is the adduct which is more deviated from the correlation line.

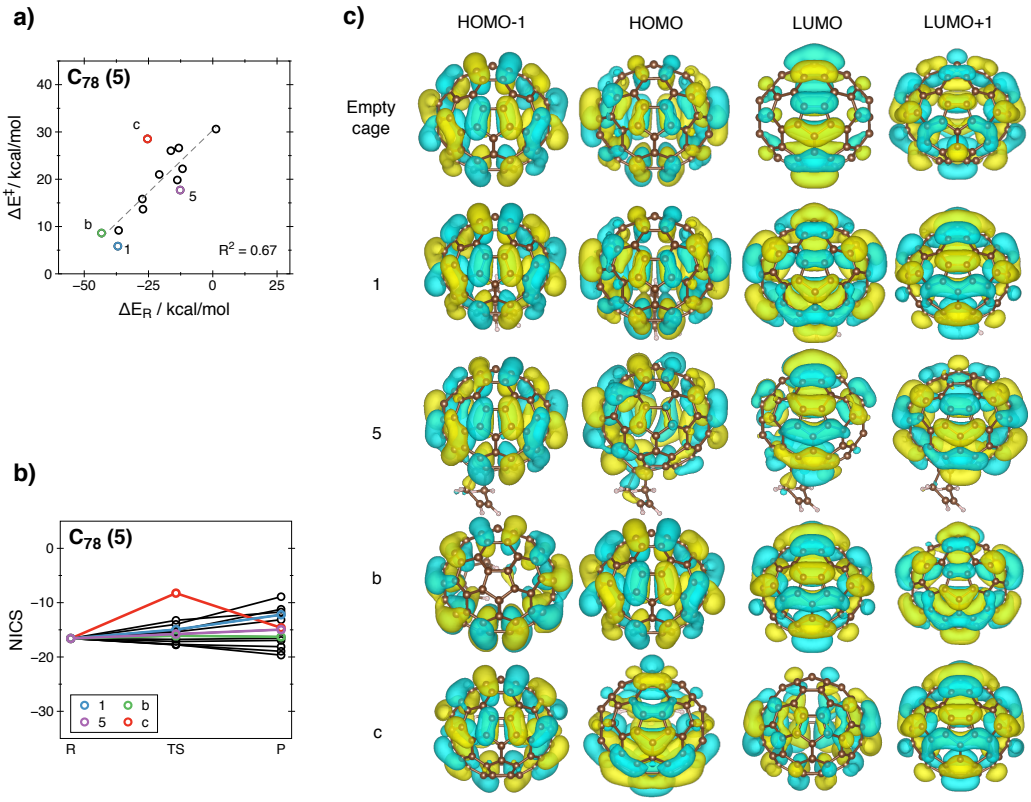

Figure S9: a) Correlation between reaction energies and energy barriers for all possible regioadducts formed by DA addition of 1,3-butadiene with fullerene C_{78} (5). b) Evolution of the NICS value in the center of the cage during DA reaction of 1,3-butadiene with fullerene C_{78} (5) for some adducts. c) HOMO-1, HOMO, LUMO and LUMO+1 orbitals for selected adducts (**1**, **5**, **b** and **c**) and for the empty cage.

11 Complete analysis of reaction energies and energy barriers of C_{80} (2) considering reactant complexes

Table S3: Energy of formation of the reactant complex (ΔE_{RC}), energy barrier from reactants ($\Delta E_1^{\ddagger}$) and reactant complex ($\Delta E_2^{\ddagger}$) and reaction energy (ΔE_R) for all possible adducts of DA addition on C_{80} (2) fullerene.

Isomer	ΔE_{RC} **(kcal/mol)**	$\Delta E_1^{\ddagger}$ **(kcal/mol)**	$\Delta E_2^{\ddagger}$ **(kcal/mol)**	ΔE_R **(kcal/mol)**
1	-3.3	8.5	11.8	-38.2
2	-3.1	7.4	10.4	-41.1
3	-3.1	8.6	11.7	-39.4
4	-2.9	11.7	14.6	-36.7
5	-3.0	15.6	18.5	-24.2
6	-2.7	14.1	16.8	-26.0
7	-3.0	15.7	18.7	-24.1
8	-2.7	13.8	16.5	-28.8
9	-3.2	13.6	16.8	-29.1
10	-2.6	13.1	15.7	-28.9
11	-2.3	18.0	20.2	-26.5
12	-1.8	17.0	18.8	-30.4
13	25.1	34.1	9.0	-16.8
14	-2.9	19.7	22.6	-18.2
15	-2.2	18.6	20.8	-25.1
16	-2.6	30.5	33.1	-12.3
17	-3.0	17.1	20.1	-17.6
18	-2.2	19.7	21.9	-24.1
19	25.7	35.5	9.9	-15.5
20	-1.8	26.3	28.1	-7.0
21	-2.5	21.7	24.2	-17.6
22	-2.6	22.2	24.8	-13.1
23	-2.6	21.7	24.3	-18.4
24	-3.1	21.4	24.5	-16.5
25	-3.1	28.3	31.4	0.1
26	-1.3	23.6	24.9	-13.7
27	-1.7	24.1	25.8	-12.3
28	-3.1	28.4	31.4	-0.1
29	-1.2	35.2	36.4	9.2
30	22.9	47.9	25.0	13.2
31	-1.5	40.0	41.5	17.9

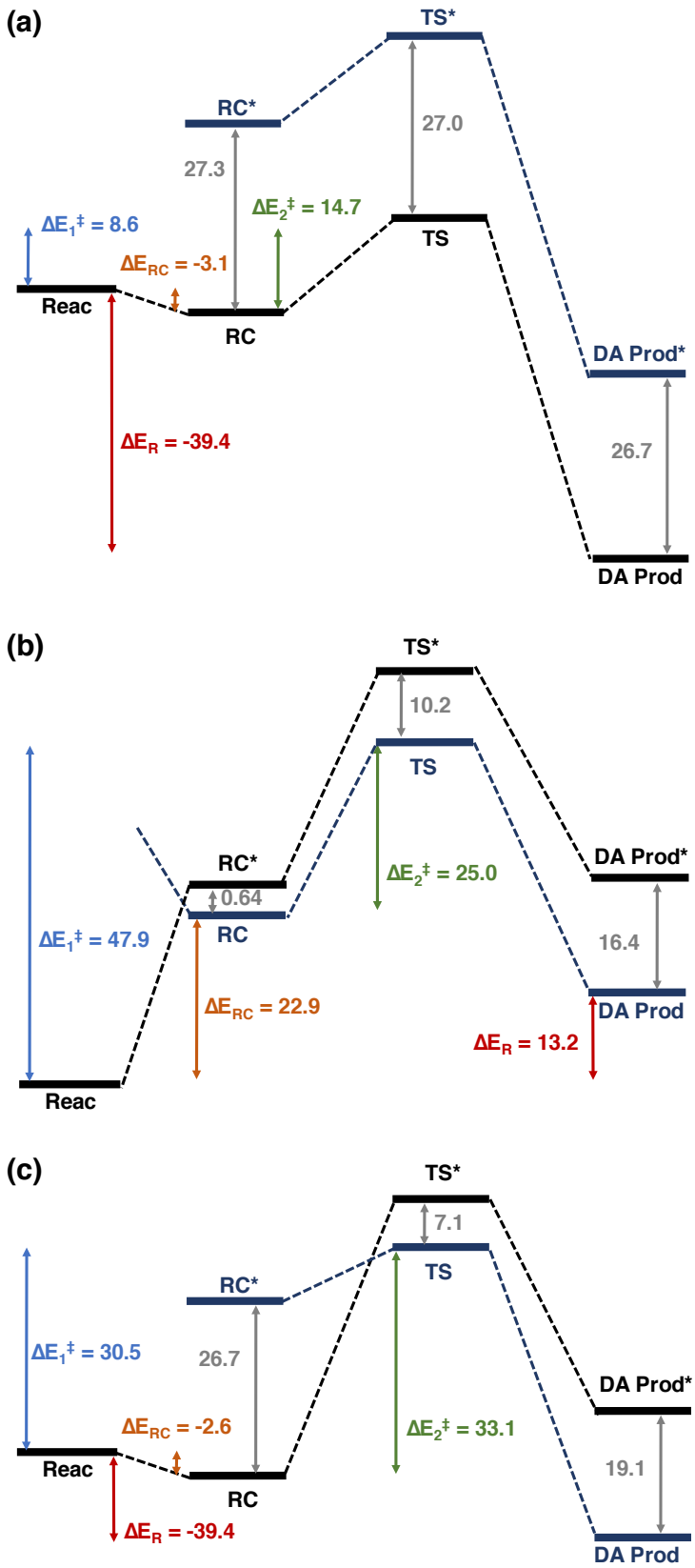

Figure S10: Energy diagrams for the DA reaction on C_{80} (2) of a) normal behavior adduct (**3**), b) one with high energy reactant complex (**30**) and c) one with high energy barrier (**16**).

References

[1] Y. Zhao and D. G. Thuhlar, *Theor. Chem. Acc.*, 2008, **120**, 215–241.

[2] Gaussian 09, Revision E.01, M. J. Frisch, G. W. Trucks, H. B. Schlegel, G. E. Scuseria, M. A. Robb, J. R. Cheeseman, G. Scalmani, V. Barone, B. Mennucci, G. A. Petersson, H. Nakatsuji, M. Caricato, X. Li, H. P. Hratchian, A. F. Izmaylov, J. Bloino, G. Zheng, J. L. Sonnenberg, M. Hada, M. Ehara, K. Toyota, R. Fukuda, J. Hasegawa, M. Ishida, T. Nakajima, Y. Honda, O. Kitao, H. Nakai, T. Vreven, J. A. Montgomery, Jr., J. E. Peralta, F. Ogliaro, M. Bearpark, J. J. Heyd, E. Brothers, K. N. Kudin, V. N. Staroverov, T. Keith, R. Kobayashi, J. Normand, K. Raghavachari, A. Rendell, J. C. Burant, S. S. Iyengar, J. Tomasi, M. Cossi, N. Rega, J. M. Millam, M. Klene, J. E. Knox, J. B. Cross, V. Bakken, C. Adamo, J. Jaramillo, R. Gomperts, R. E. Stratmann, O. Yazyev, A. J. Austin, R. Cammi, C. Pomelli, J. W. Ochterski, R. L. Martin, K. Morokuma, V. G. Zakrzewski, G. A. Voth, P. Salvador, J. J. Dannenberg, S. Dapprich, A. D. Daniels, O. Farkas, J. B. Foresman, J. V. Ortiz, J. Cioslowski, and D. J. Fox, Gaussian, Inc., Wallingford CT, 2013..

[3] Y. Wang, *Physical Chemistry Chemical Physics*, 2018, **20**, 13792–13809.

[4] P. Fowler and D. E. Manolopoulos, *An Atlas of Fullerenes*, Clarendon Press, Oxford, U.K., 1995.

[5] X.-F. Gao, C.-X. Cui and Y.-J. Liu, *J. Phys. Org. Chem.*, 2012, **25**, 850–855.

[6] S. Osuna, R. Valencia, A. Rodríguez-Fortea, M. Swart, M. Solà and J. M. Poblet, *Chem. Eur. J.*, 2012, **18**, 8944–8956.